JOINT INSTITUTE FOR NUCLEAR RESEARCH, DUBNA
Report P1 - 7892

MEASUREMENT OF THE POSITIVE MUON'S LIFETIME

M.P. Balandin, V.M. Grebenyuk, V.G. Zinov
A.D. Konin and A.N. Ponomarev

Dubna 1974

Translated at CERN by R. Luther
(Original: Russian)
Not revised by the Translation Service

(CERN Trans. 74-9)

Geneva
September 1974

Introduction

Sent to JETP

The first relatively accurate measurements of the positive muon's lifetime $(0.1 \pm 0.05)\%$ were carried out in 1962-1963 /1-4/ but no further progress was made for a long time. The paper by R.W. and D.L. Williams added little to the experimental accuracy already achieved, and it was only the change in measuring technique proposed by Duclos et al. /6/ that pushed research forward.

All the papers reveal certain substantial systematic limitations to the accuracy with which the muon's lifetime is measured. The conventional apparatus used for detecting positrons from muon decay has a small solid angle. This reduces the data acquisition rate and makes it difficult to select useful events by comparing the positrons which are detected with the muon at rest. Background events can slip in in many ways. The small solid angle also creates another difficulty. Allowance has to be made for the possible effect of asymmetry in the outgoing positrons. Therefore, the residual magnetic field where the muon is stopped must be reduced to hundredths or thousandths of an oersted.

Moreover, the fact that the decay positrons are very energetic has not yet been sufficiently exploited.

Method of measurement

The method used by us is based on the idea of 4π - positron detection using a Cherenkov detector. In this way the data acquisition rate was increased, the background reduced and the effect caused by the asymmetrical emergence of the positrons is suppressed.

Device

The measurements were carried out in the meson beam-line of the JINR synchrocyclotron. A pure beam of 130 MeV/c muons was used. The muons were selected from the backward decay of pions captured in the beam line.

Fig. 1 shows a block diagram of the experiment. Scintillation counters 1 and 2, measuring 10 x 10 x 1 cm, are used to record the incident muons. A water threshold Cherenkov counter is used to record the positrons only. The muons' energy was selected so that they remained in the centre of the Cherenkov detector's volume. The solid angle for positron detection is thus 4 π.

The dimensions of the radiator (Ø 30 x 30 cm) are selected so that the incident muons do not radiate Cherenkov light and the positron recording efficiency remains high. This prevents the muon stop signal from affecting the time position of the outgoing positron's signal. Two FEU-49 photomultipliers scan the entire volume of the water radiator with its diffusely reflecting layer of MgO (fig. 2). The photomultipliers are selected so that their photocathodes' sensitivity is both high and well-matched. Sheet Permalloy was used to screen the photomultipliers and the radiator volume from the magnetic field. The whole structure was housed inside a steel cylinder 1 m long. A copper-wire solenoid is wound over the steel screen in order to provide active d.c. compensation for the remanent magnetic field. The field was concentrated at 0.01 oe by means of a built-in Permalloy detector.

A lead collimator Ø 9 cm was placed at the point where the muons entered the Cherenkov counter, and a window was cut in the steel screen.

Selection of conditions for measurement

As in other papers, only those events were selected in which just one muon (the start muon) and one positron appeared during the gating pulse. In this case the decay curve is described by a very simple formula (A exp $(-\lambda t)+$ B), where t is the time, λ - the decay rate, and A and B are constants.

As the calculations showed, there are optimum conditions for measurements depending on the intensity of the muon stops and the length of the interval during which positrons are detected. Fig. 3 shows the results of the calculations in graph form.

It is interesting to note that with this method the accuracy with which the muon's lifetime can be measured is limited to about 10^{-5}. The method must be changed in order to improve on this.

At a muon intensity of $7 \cdot 10^{3}$ sec^{-1}, not allowing for the duty factor, the full gate width was 20 μsec. The zero moment for the appearance of positrons in relation to the muon stop is shifted 5 μsec on the time scale. This reduces the possible effect of transient processes caused by signals from particles passing through the detectors before the gates are opened.

Electronics

Fig. 4 shows a simplified block diagram of the electronics system. Counters 1 and 2 picked out the incoming muon (C1 coincidences). Counters 3 and 4 identified the decay positron. The amplifiers in counter channels 3 and 4 were adjusted so that signals from the same flash were equal in height. During runs the counting rate in these channels was also the same. The following action was taken in order to improve the uniformity of the positron detection efficiency. Firstly, coincidences 3 and 4 were selected (circuit C3) so that the energy threshold for positron detection could be reduced without interference from the photomultipliers. Secondly, discriminator D5 following linear adder LA was used to select those events in which, for instance, one of the pulses from photomultipliers 3 and 4 was large. This may occur when the positron emerges in the direction of one of the photomultipliers, and a large part of the light cone falls on its photocathode.

The multiple event detection circuits (ME1 and ME2) allowed the time-code converter (TC) to select events when a second muon or positron did not appear whilst the gate was open. Delay line DL-2 shifted the positron signal ("Stop") 5 μsec. in relation to the muon stop signal ("Start"), i.e. it shifted the beginning of the exponential. Delay line DL-1 (also 5 μsec.) was used in the same way to reject events where a second muon arrived during the gating pulse.

In order to exclude transient effects caused by the intensity-related shift in the d.c. level, all electronic connections were galvanic. Where this was impossible, bipolar signals were produced.

Time-code converter

The time-code converter forms a major part of the apparatus. It was specially designed for the experiment. It therefore includes certain special features. Fig. 5 shows a simplified block diagram of the converter. The start pulse (stopped muon) triggers flip-flops F1 and F2. Signals from the crystal oscillator CO pass to registers R1 and R2a via gating circuits C1 and C2 respectively. The "stop" pulse (decay positron) returns flip-flop F2 to its original state, and the digital code of the time interval is recorded on register R2a. Flip-flop F1 returns to its original state only after a given number of pulses has been accumulated in register R1, i.e. it sets the gate width by digital means. During the gate interval, event pulses (arrival of second muon, second positron) may be transmitted via gating circuit C3 to register R2b at any time. In the event code 10 bits (R2a) are assigned to time and 2 bits (R2b) to characteristics. At the end of the gating pulse, the event code is transmitted to the AI-4096 memory in the measuring centre of the Laboratory for Nuclear Problems where the events are sorted and stored.

The frequency of the crystal oscillator was approximately 50 MHz (its absolute value was known to an accuracy of 100 Hz).

Checking the operation of the apparatus

In order to achieve high measurement accuracy, the operation of the apparatus must be checked. The main criterion is the differential non-linearity of the whole electronics system from the counters through to the time-code converter. Non-linearity may be caused both by coupling between the start-stop channels and by the superposition of pulses in each channel. If the mean differential non-linearity of the electronics system is represented in the form

$(C + D \lambda t)$, it then follows from the estimates that the D/C ratio is equal to the relative error in the lifetime measurements.

The differential non-linearity of the apparatus was measured in conditions similar to the operating conditions. The signals from two scintillation counters, which recorded γ-quanta from radioactive sources, were transmitted to the system's inputs. After several days of measurements, it was found that the mean differential non-linearity of the whole system disappears at $D/C = \pm 10^{-5}$. Fig. 6 shows the intermediate results from the tests which clearly demonstrate the quality of the electronics system.

The time resolution of the Cherenkov detector at 10^{-4} from the maximum is 100 nsec. (fig. 7). According to the results from the runs, the decay positrons were detected with 90% efficiency.

Measurements and processing of results

The measurements were carried out during 4 runs on the synchrocyclotron on different days. During operation, the data were transmitted through a direct link to the computer every 2 hours. Rapid processing was then carried out using simplified programs. The results were presented in both digital and graphic form.

At the end of the run the time spectra were processed in full using the χ^2 minimum method. When the parameters were varied, both the background part and the useful part of the spectrum were t aken into account by means of the formulae $(C \exp(-\lambda t) + B)_t < 0$ and $(A \exp(-\lambda t) + B)\ t > 0$. The results coincided when the background and useful parts of the spectrum were processed separately within the limits of error. The first time spectrum channel was shifted 320 nsec. from the beginning of the exponential.

The results are shown in the table. The muon lifetime value ($2.19711 \pm 0.00008\ \mu$sec) is corrected once to allow for the final resolution of the circuits which identify events with two muons or two positrons. The relative value of the correction is approximately 10^{-5}.

One hundred hours of physics yielded 10^9 useful events.

The accuracy of the set-up used by Duclos et al. /6/ may be improved still further by increasing the speed of response of the positron detectors and by extending their solid angle to 4 π .

In conclusion, the authors are deeply grateful to A.I. Mukhin for useful discussions, to L.I. Lapidus for his continued interest and support, to S.V. Medved' for helping to perfect the measuring system, to V.I. Komarov, S.M. Korenchenko and V.S. Roganov for their helpful advice, and to M.M. Petrovskij for helping with the construction of the apparatus.

Bibliography

1. F.J.M. Farley, T. Massam, T. Muller and A. Zichichi. Proc. 1962 Int. Conf. on High Energy Physics at CERN, p. 415.
2. R.A. Lundy. Phys. Rev., 125, 1936 (1962).
3. M. Eckhause, T.A. Fillipas, R.B. Sutton and R.E. Welsh. Phys. Rev., 132, 422 (1963).
4. S.L. Meyer, E.W. Anderson, E. Bleser, L.M. Lederman, J.L. Rosen, J. Rothberg, I.-T. Wang. Phys. Rev., 132, 2693 (1963).
5. R.W. Williams and D.L. Williams. Phys. Rev. D6, 737 (1972).
6. J. Duclos, A. Magnon and J. Picard, Phys. Lett., 47B, 491 (1973).

The manuscript was received by the publishing department on 25 April 1974.

Table

Run	Lifetime (μsec)	$\chi^2/\langle\chi^2\rangle$
1	2.19740 ± 0.00031	0.82
2	2.19687 ± 0.00014	1.02
3	2.19731 ± 0.00014	1.18
4	2.19709 ± 0.00013	0.87
Total spectrum	2.19711 ± 0.00008	0.87
Paper /6/	2.1973 ± 0.0003	

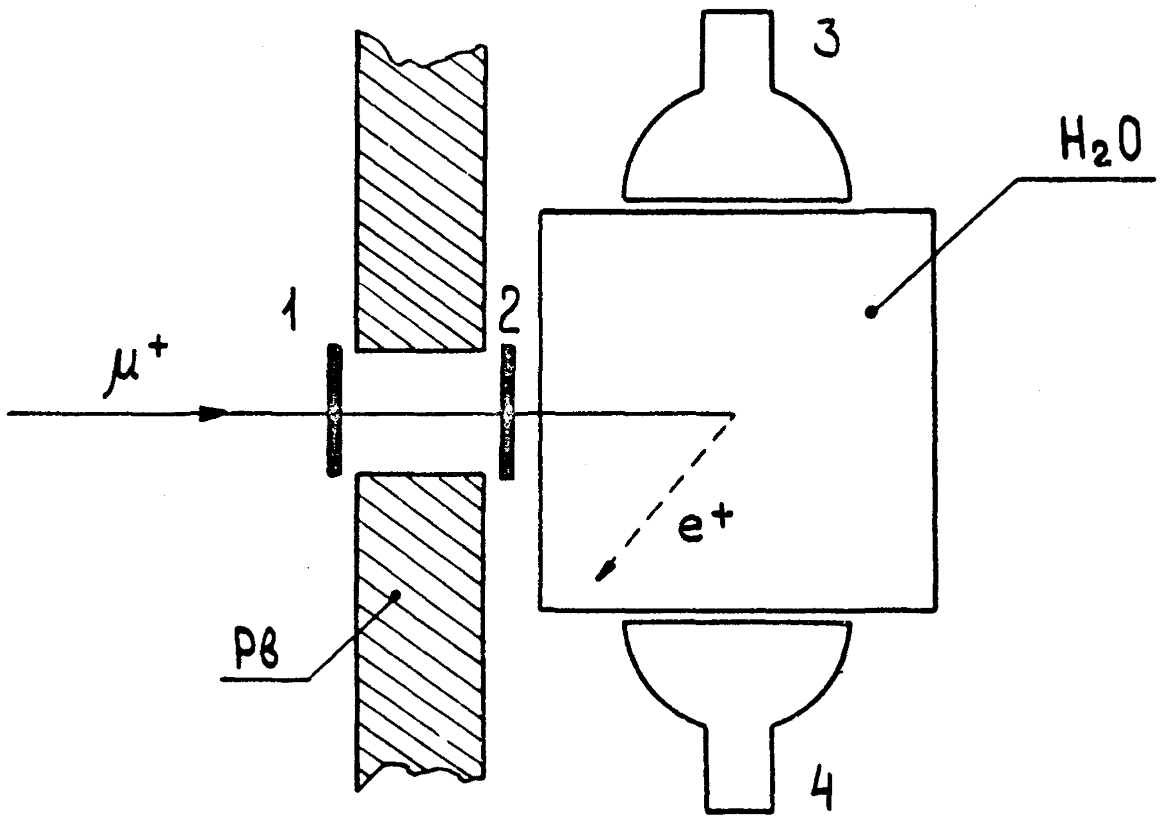

Fig. 1. Block diagram of the experiment.

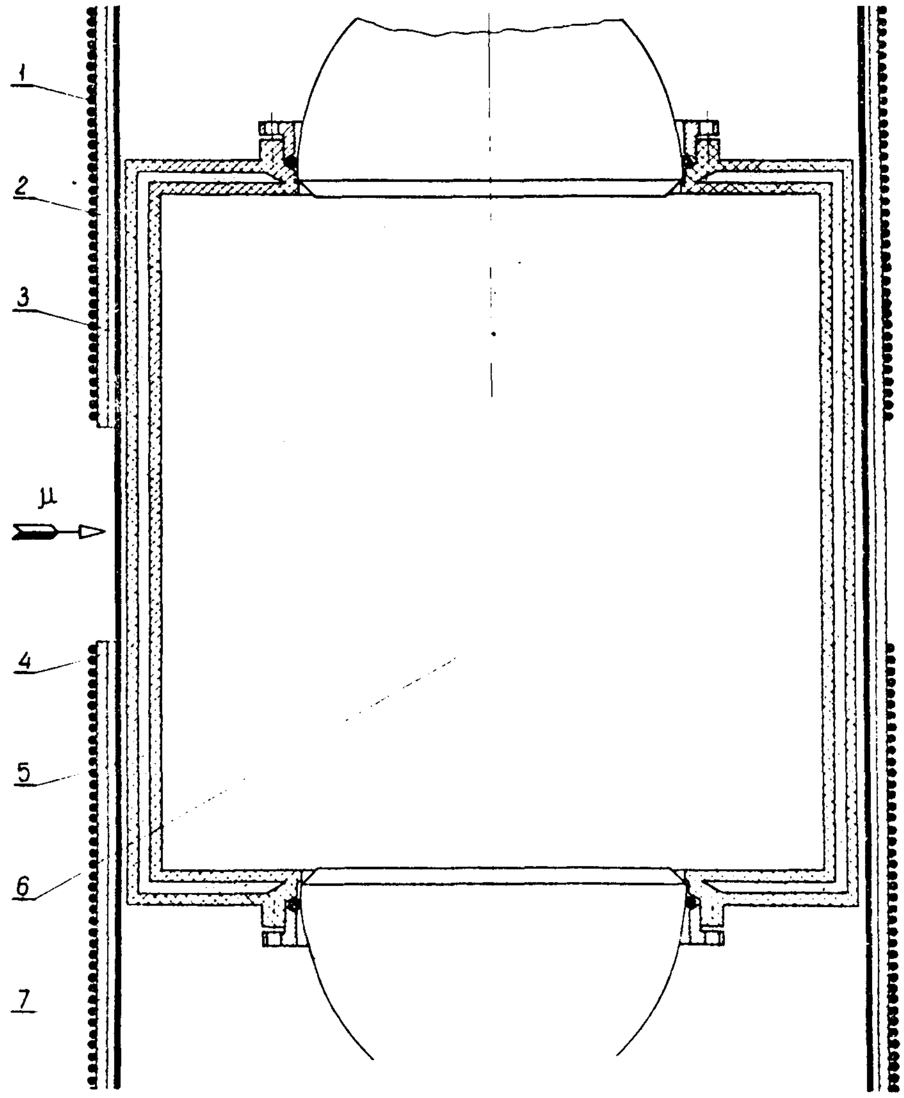

Fig. 2. Structure of the Cherenkov counter:
1. winding for compensating the magnet field;
2. steel magnetic screen;
3. Permalloy magnetic screen;
4. Perspex radiator walls;
5. MgO light reflector;
6. water;
7. photomultiplier.

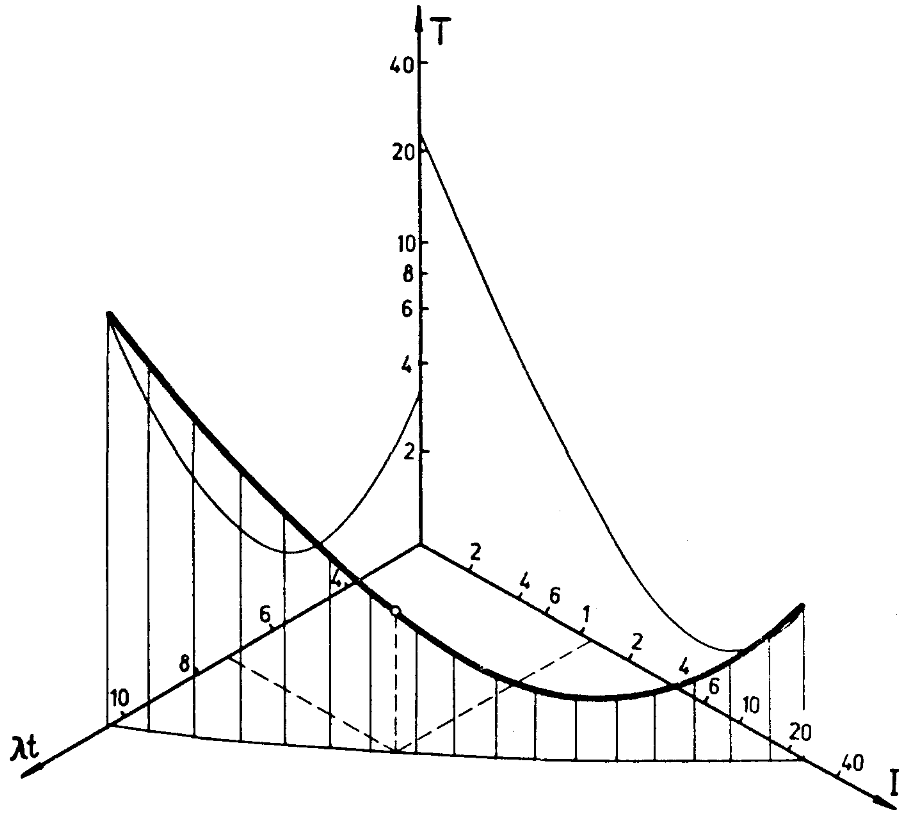

Fig. 3. Optimum intensity graph.
t - gate width; T - measuring time;
I - stopped muon intensity.

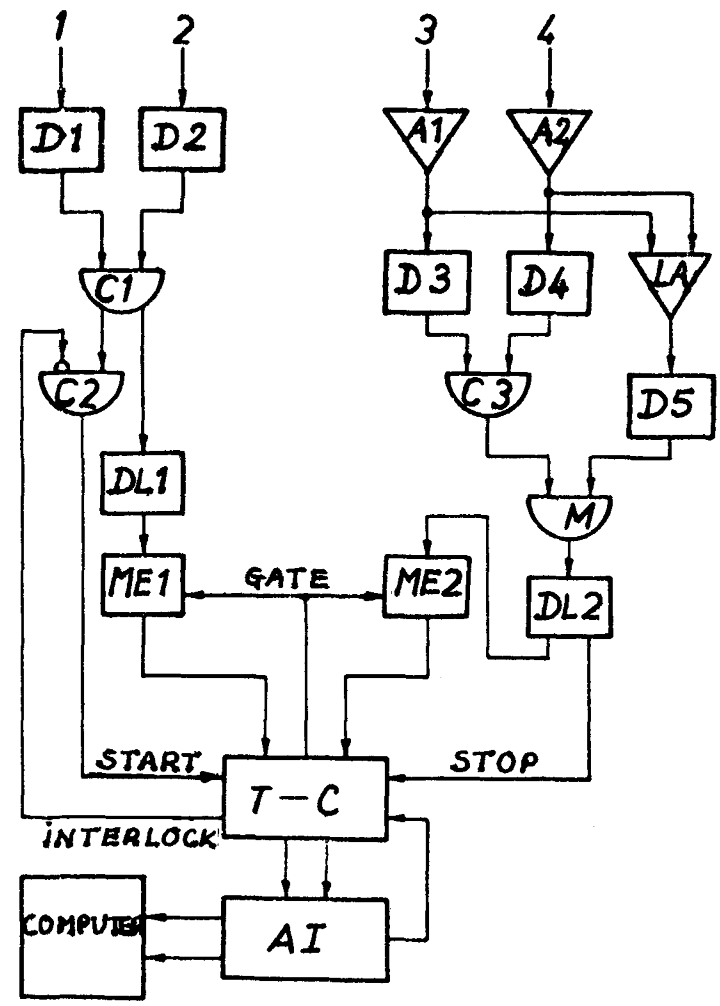

Fig. 4. Block diagram of the electronic system; D - discriminator, C - coincidence circuit, M - mixer, DL - delay line, LA - linear adder, A - amplifier, TC - time-code converter, ME - circuit for detecting a second pulse in the gates, AI - AI4096 buffer store.

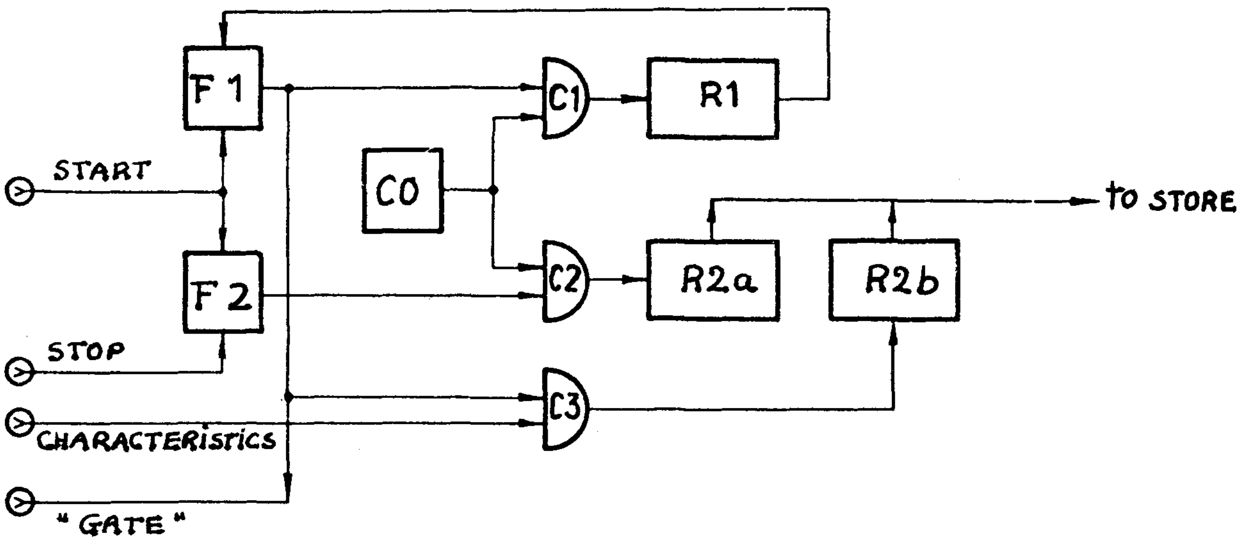

Fig. 5. Block diagram of the time-code converter:
F - flip flop, CO - crystal oscillator,
C - coincidence circuit, R - register.

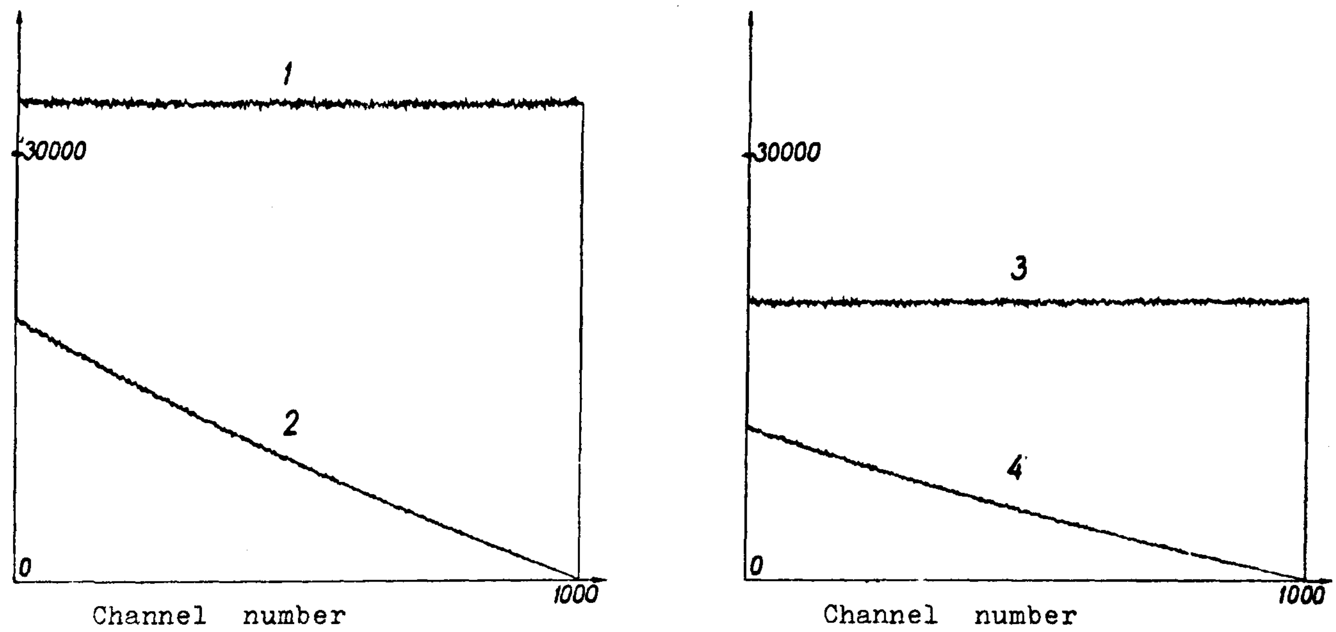

Fig. 6. Time spectra: 1. 1 'start' pulse and 1 'stop' pulse in the gate; 2. 1 'start', 2 'stop'; 3. 2 'start', 1 'stop'; 4. 2 'start', 2 'stop'.

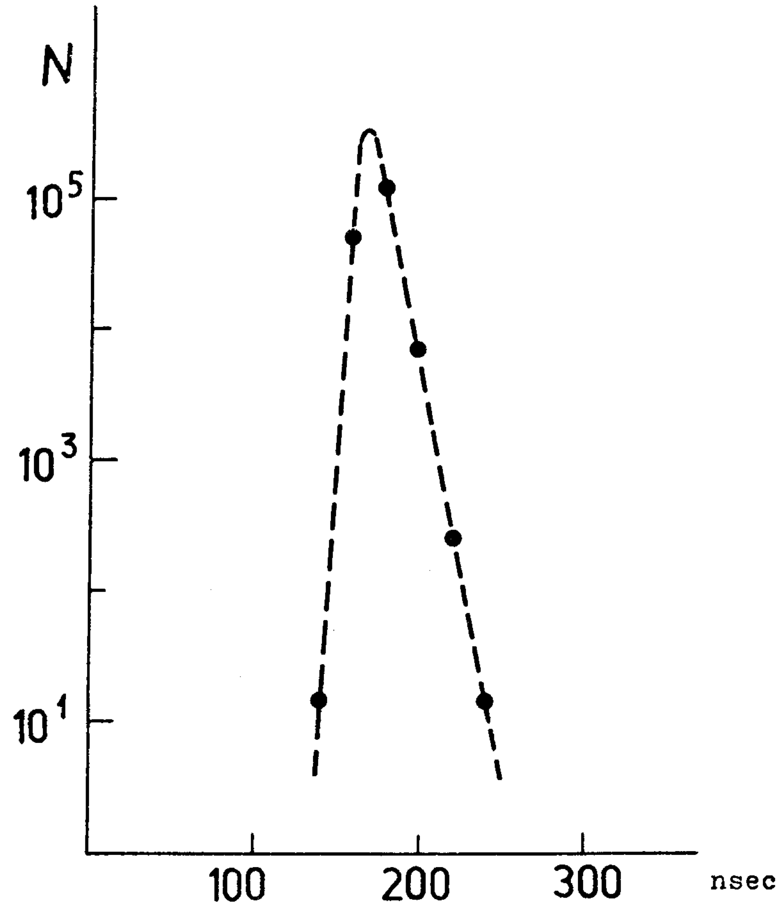

Fig. 7. Time resolution of the apparatus.

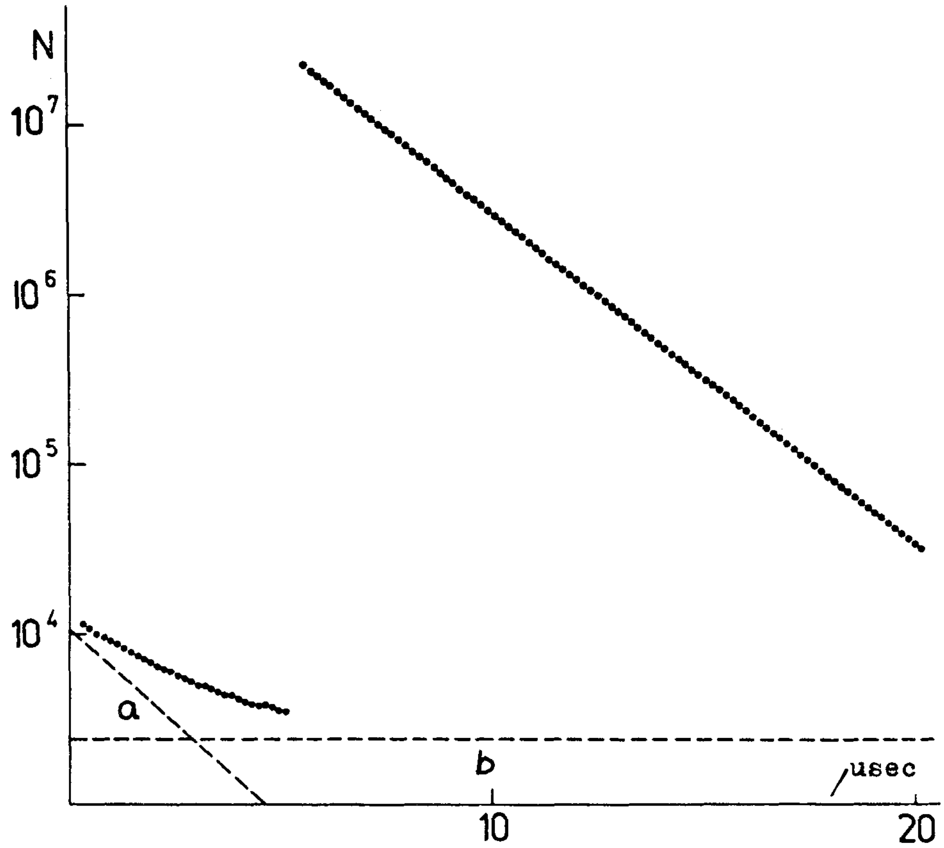

Fig. 8. Decay curve (for one run).